

Large Resonators Designed by the Wave Filter Theory

In the Wave Filter Theory, a rectangular resonator as shown in Fig.1 is assumed. Based on the theory (Nakamura et al 1996), we can estimate the necessary dimensions of l_2 , l_1 and b_3 for given b_0 and the required effective frequency band as follows.

$$\left. \begin{aligned}
 b_3 &= \frac{mb_0}{\sqrt{2(1-m^2)}} \\
 l_2 &= \frac{1}{\pi f_c} \sqrt{\frac{gh(1-m^2)}{2}} \\
 l_1 &= \frac{m\sqrt{gh}}{2\pi f_c}
 \end{aligned} \right\} \quad (1)$$

where g is the gravitational acceleration, h is a water depth, and m is a function of the critical frequency f_c and the pole frequency f_∞ of an effective frequency band ($f_c < f < f_\infty$) of a wave resonator and is given by

$$m = \sqrt{1 - \left(\frac{f_c}{f_\infty}\right)^2} \quad (2)$$

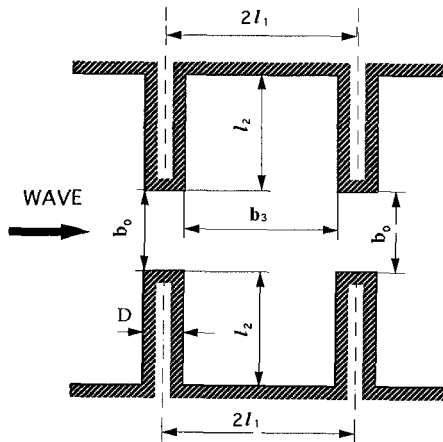


Fig.1 Definition sketch of a resonator.

Table 1 Design conditions and results of a resonator.

TYPE	b_0	$T_{\infty}(=1/f_{\infty})$	$T_c(=1/f_c)$	b_3	l_2	D	b_3/l_2	h
(A)	310m	43s	80s	344m	166m	26m	2.07	30m
(B)	600m	81s	135s	566m	312m	30m	1.82	30m
(C)	300m	65s	180s	550m	159m	30m	3.50	12m

The pole frequency f_{∞} corresponds to a frequency at which wave transmission through a resonator becomes the lowest.

Table 1 shows typical results on the horizontal dimensions of resonators for various design conditions. Resonators with a wide entrance are presumed for passing ships. The aspect ratio of a resonant basin of these resonators, b_3/l_2 , ranges from 1.8 to 3.5. Valembois (1953) pointed out that the aspect ratio of the resonant basin should be about 2 for the effective protection.

Effects of the Aspect Ratio of a Resonant Basin on the Wave Transmission

To examine the effectiveness of the designed resonators specified in Table 1, we calculated wave transmission characteristics through a linear array of the resonators by the vertical line source Green's function method (Nakamura 1994). This numerical method takes into account the effect of an infinite array of bodies by considering an infinite number of mirror image sources. In the computation, the reflection coefficient of the wall of resonators is assumed to be 0.8 for modeling the practical situations.

Figs. 2~4 show the computation results on the wave transmission through an infinite array of the resonators, Type(A), (B) and (C) in Table 1, respectively. The wave transmission characteristic is specified by the wave height ratio K_T , which is defined by

$$K_T = (H_T)_{rms} / H \quad (3)$$

where $(H_T)_{rms}$ is a root-mean-square value of transmitted wave height along the array direction, and H is an incident wave height. The rms value of transmitted wave height is necessary to account for the short-crested wave pattern about an array of resonators, especially under the condition $\lambda/L > 1$ (λ : center-to-center distance between the adjacent resonators, L : wave length). It has become known that wave patterns about an infinite array of identical bodies under the condition $\lambda/L > 1$ are short-crested even though in the region far from the array (Dalrymple & Martin 1990 and Nakamura 1994). In other condition $\lambda/L < 1$, the wave pattern is long-crested and the definition of K_T coincides with that of a well known transmission coefficient.

From these figures, it is seen that the value of K_T for each array of resonators, Type (A), (B) and (C), is comparatively small for the presumed effective range of wave period as shown in Table 1. The spike-like variation of K_T is due to the wave resonance in the transverse direction. Under the transverse resonant condition, a center-to-center length of the adjacent resonators λ is equal to a wave length L . In the numerical computation, this resonant condition corresponds to the singular point at where one of eigenfunctions of the Green's function becomes indefinite.

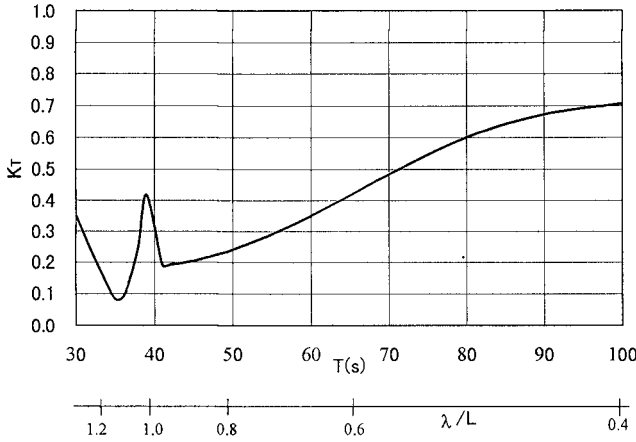


Fig.2 Dimensionless transmitted wave height through the arrayed resonators of Type (A) ; water depth $h=30$ m.

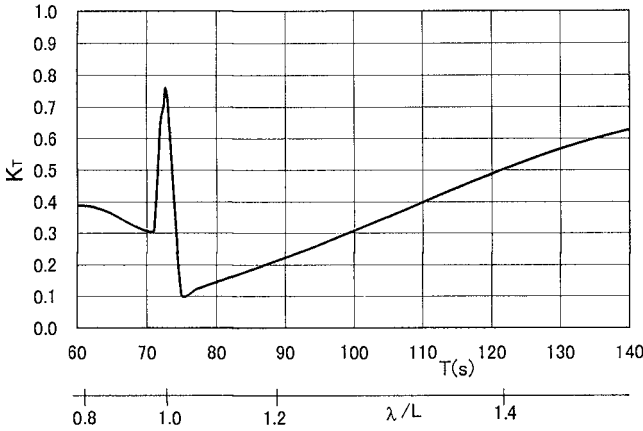


Fig.3 Dimensionless transmitted wave height through the arrayed resonators of Type (B) ; water depth $h=30$ m.

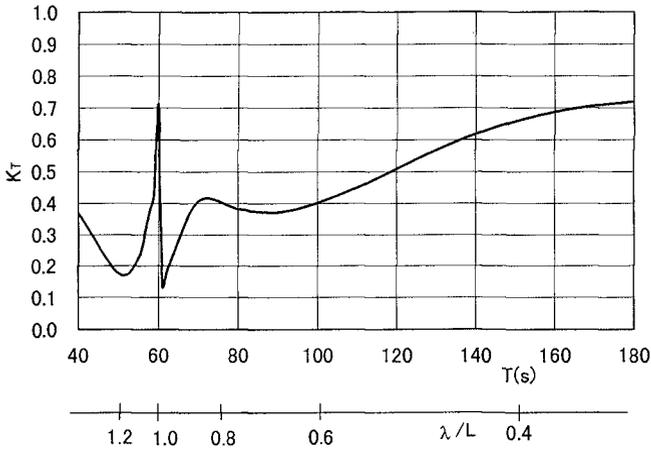


Fig.4 Dimensionless transmitted wave height through the arrayed resonators of Type (C) ; water depth $h=12\text{m}$.

From inter-comparison among these figures, we can see some difference with the performance of the resonators. For instance, Type (A) and (B) resonators show the much lower K_T value than Type (C) resonator in the presumed effective wave period range. It may be caused by the difference of aspect ratios of a resonant basin b_3/l_2 . The aspect ratio is about 2 for Type(A) and (B) resonators, which is equal to the aspect ratio recommended by Valembois (1953). On the other hand, the aspect-ratio of Type (C) resonator is 3.5. Therefore, it is better to design a resonator in such a way that the aspect ratio of a resonant basin is about 2. However, it is noted that the entrance width b_0 of a resonator is also an important factor to determine the performance.

As a result, we can use the Wave Filter Theory to get a rough estimate of geometrical dimensions of a wave resonator that is effective for the given frequency range. However, it is hard to know the degree of effectiveness of the resonator by the theory. In this case, we have to rely on the numerical computation method.

Experimental Results in a Channel for Regular and Irregular Waves

In order to check the validity of the design results by the Wave Filter Theory, we carried out model tests in a long channel. The channel is 1.2m high, 1m wide and 26m long. The distorted model was applied to avoid the difficulties arising from the wave nonlinearities. The model scale is 1/324 in the horizontal dimensions and 1/167 in the vertical dimension. Type (A) resonator in Table 1 was basically used. The setup of a model resonator is shown in Fig.5. Considering the mirror image effect of both side walls, only a half of the resonator was placed in a long channel. The wave field in this channel is equivalent to the one around an infinite array of identical resonators when the wave reflection from side walls is perfect. In the experiment, the allocation pitch length λ of the arrayed resonators is equal to double of a channel width, i.e. 2m.

We used two different types of model resonators with the same dimensions, but having different reflection characteristics. One model is made of plywood and has a high reflective

nature. The other model consists of low-reflective walls covered with porous materials on the surface. It was confirmed by the other experiment that the reflection coefficient of the low-reflective wall is approximately 0.8.

In order to be able to analyze the short-crested wave pattern around a resonator in the channel, we set a linear array of five wave gauges in the transverse direction to measure transmitted waves through a resonator. Wave conditions used in the experiment are largely classified into two categories, i.e. regular and irregular waves.

In the case of regular waves, wave period T_m ranges from 1.2 s to 3.5s (in prototype scale $T=22\sim64$ s) and wave height H_m is fixed at about 3cm (in prototype scale $H=5$ m).

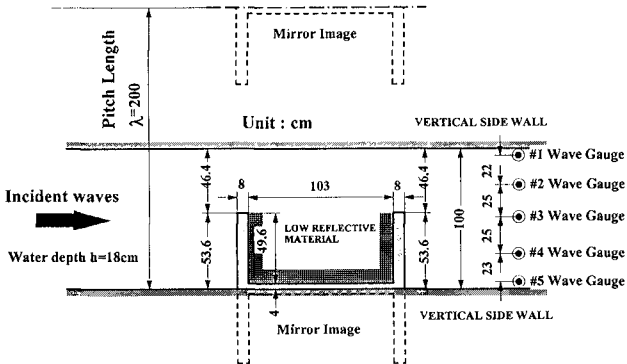


Fig.5 Experimental setup; Type (A) resonator.
(In case of low reflective walls)

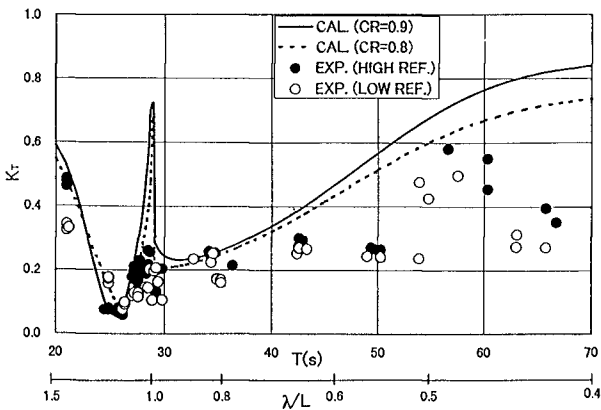


Fig.6 Dimensionless transmitted wave height through the arrayed resonator for regular waves.

For the case of irregular waves, the Bretschneider spectrum was used as a target frequency spectrum. At present, the frequency characteristic of infragravity waves has not been clarified. Therefore, we just account for the irregular nature of wave trains in the field.

Fig.6 shows typical results for regular waves, where the rms transmitted wave height ratio K_T is plotted as a function of wave period T in the prototype scale. The parameter λ/L is also plotted as a second horizontal axis.

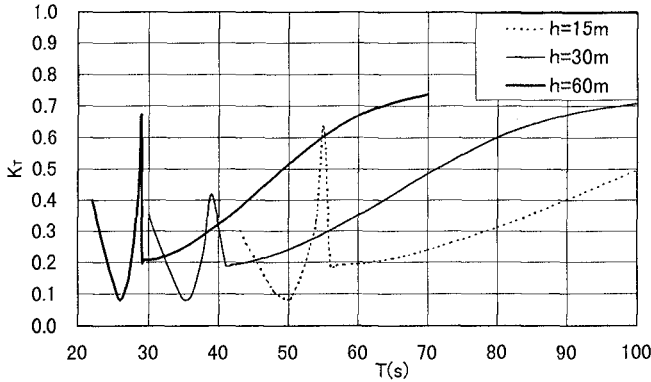


Fig.7 Variations of K_T of Type(A) resonator with water depth.

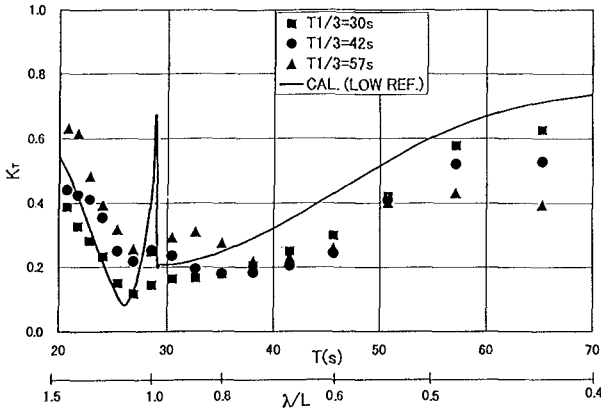


Fig.8 Dimensionless transmitted wave height through the arrayed resonator for irregular waves.

In the figure, two different results are shown. One is for the resonator consisting of high reflective walls and the other consists of dissipative walls covered with porous materials. Further, in the figure, the computed result by the Green's function method is also plotted. In the computations, the distorted model was used as a real structure. Hence the water depth is assumed to be 60m in the prototype scale.

Except the condition near the transverse resonance at $\lambda/L=1$, we can see the reasonable agreement between the computed and experimental results. However, for longer wave period conditions, the measured value of K_T is smaller than the computed one. It may be partly caused by the frictional damping on the sea bed.

From the comparison between the two experimental results for the low- and high-reflective wall cases, it is seen that there is little influence of the different wall types on the wave transmission.

Fig. 7 shows the effect of water depth on the performance of resonators. In the figure, the computed results of K_T for the arrayed resonators with the same horizontal dimensions (Type (A)), but for three different water depths, are shown. It is apparent that the effective range of wave period shifts to the side of longer waves with decreasing water depth h . This is caused by the decrease of wave length with water depth. This tendency can also be predicted by Eq.(1).

Fig. 8 shows the result of K_T for irregular waves with different significant wave periods $T_{1/3}$, where K_T is defined as a transfer function in the frequency domain. We can see the similar tendency to the result of regular waves. From the examinations described above, we can say that the large resonator is effective for reducing very long waves of both regular and irregular wave trains.

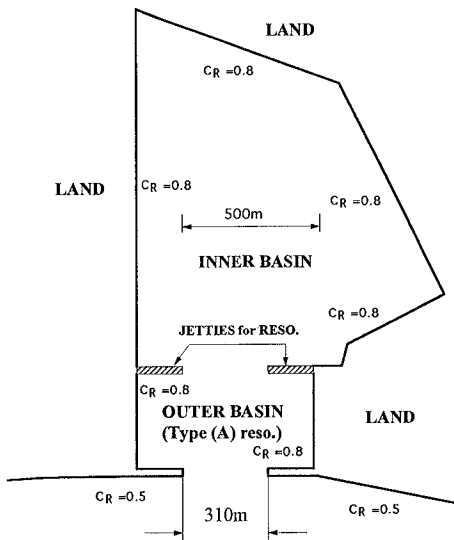


Fig.9 Layout of a model harbor and reflection coefficients on the boundary.

Numerical Experiment on the Harbor Tranquility

In order to confirm the effectiveness of the resonator as an outer harbor of a double-basin type, we carried out numerical experiments based on the vertical line source Green's function method (Isaacson 1978 and Nakamura et al 1985).

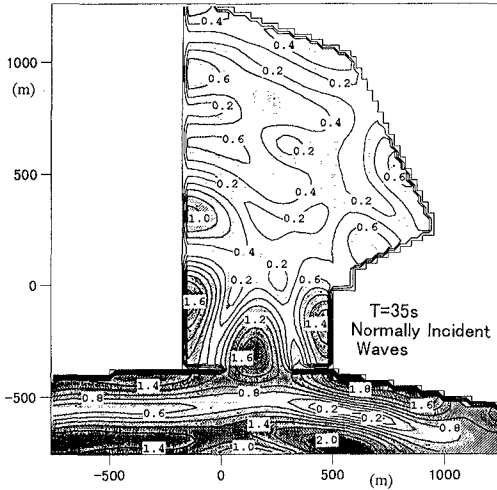


Fig.10 Wave height distributions around the original harbor ($T=35s$, normal incidence).

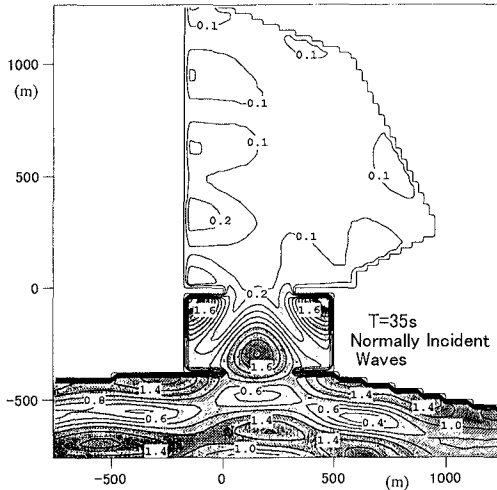


Fig.11 Wave height distributions around the harbor with a resonator ($T=35s$, normal incidence).

Fig 9 shows a layout of an original harbor adopted in the numerical experiment. It is assumed that the water depth h is constant around the harbor and is equal to 30m. Reflection characteristics of harbor boundaries are specified in the figure by the reflection coefficients C_R . When we add two jetties in a harbor as shown in dashed lines in the figure, the harbor becomes a double-basin type with the resonator of Type (A) as an outer basin.

Fig. 10 and 11 show the comparisons of wave height distributions between two different models, i.e., the original harbor and the one with the type (A) resonator as an outer harbor as seen in Fig 9, respectively. In these figures, the dimensionless wave height ratio to an incident wave height is plotted. The normal incidence of waves to the harbor entrance is presumed.

We can see that the resonator designed by the Wave Filter Theory is very effective to reduce long-period waves incoming to the inner basin. However, we can also see a subsidiary effect of the resonator, i.e., higher waves in the resonator including at the harbor entrance. It may be thought that there is little or no influence on passing ships because of a small amplitude of very long waves. Fig 12 shows another example, where the wave period T is longer than the case of Fig. 11. It is again confirmed that the resonator plays an effective protector for incoming waves to the inner basin.

Finally, Fig 13 shows the result of wave height distributions in case of obliquely incident waves to the harbor entrance. The inclination angle is 30-degree from the normal incident direction. It can be seen that the performance of a resonator is not affected by the incident angle of waves.

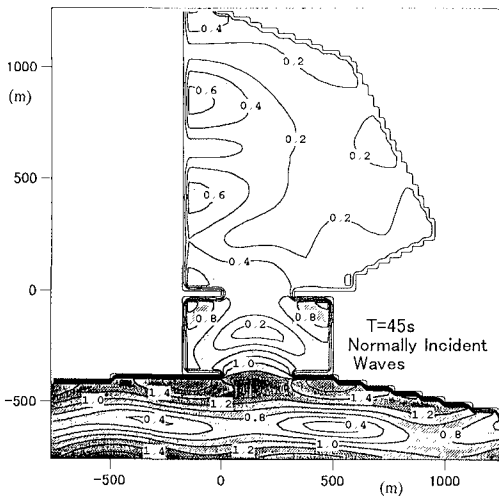


Fig.12 Wave height distributions around the harbor with a resonator ($T=45s$, normal incidence).

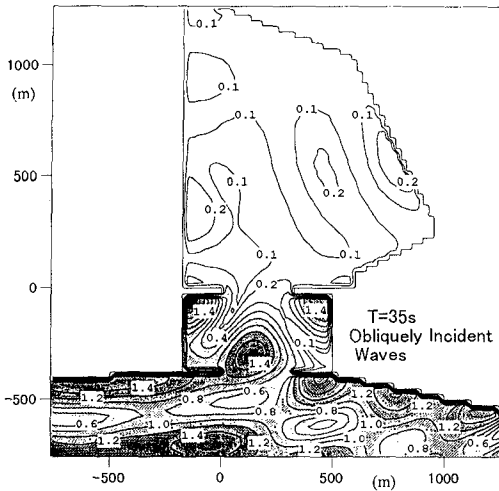


Fig.13 Wave height distributions around the harbor with a resonator ($T=35s$, oblique incidence).

Conclusion

The Wave Filter Theory is very useful to design a large resonator as the outer basin of a double-basin type harbor for protecting the inner basin from very long waves, which may cause long period motions of a moored ship at the piers. It was confirmed experimentally that the large resonator as the outer basin is effective for reducing both regular and irregular waves in the inner basin.

It is suggested that the aspect ratio of a resonant basin should be the order of 2:1 for the effective protection of the inner basin from incoming waves. However, it is noted that the entrance width of a resonator is also an important factor to determine the performance.

References

- Dalrymple, R.A. and Martin, P.A. (1990) : Wave diffraction through offshore breakwaters. *Journal of the Waterway, Port, Coastal and Ocean Engineering Division, ASCE*, Vol.116, No.6, pp.727-741.
- Isaacson, M.Q. (1978): Vertical cylinders of arbitrary section in waves. *Journal of the Waterway, Port, Coastal and Ocean Engineering Division, ASCE*, Vol.104, No.WW4, pp.309-324.
- Nakamura, T. and Oku, Y. (1985): A method of numerical analysis on wave diffractions about a vertical structure of arbitrary section, *Proc. of 32nd Japanese Conf. on Coastal Eng.*, pp.594-598.